Thermodynamic Lattice and Electronic Properties of Small Particles*

V. Novotny and P. P. M. Meincke
Department of Physics, University of Toronto, Toronto M5S-1A7, Ontario, Canada
(Received 19 April 1973)

Specific-heat measurements were performed on small lead particles (22, 37, and 60 Å) and 22 Å indium particles over the temperature range 1.5–15 K. For all sizes the enhancement of the specific heat due to the increased importance of low-frequency surface modes and attendant depletion of higher-frequency modes was observed. Although the magnitude of the observed surface-phonon specific heat agrees reasonably well with theoretical estimates at intermediate temperatures, the observed enhancements apparently are not proportional to the surface area and do not exhibit quadratic temperature dependence. The rapid decreases of the heat capacity at lowest temperature appear to be consistent with the estimates of low-frequency cutoffs in the phonon spectrum caused by quantum size effect. At temperatures around one-tenth of the bulk Debye temperature the surface specific heats exhibit maxima. Differences in the electronic specific heat in the superconducting state between small particles and the bulk were observed. The transition-temperature behavior of lead and indium particles is also discussed.

I. INTRODUCTION

Although theoretical interest in the thermodynamic lattice and electronic properties of systems with large surface areas has existed for several decades, few experimental studies have been reported because of the difficulties involved in their measurements. The primary objective of the present work was to investigate the effect of surface and size on the lattice properties of small systems by measuring the low-temperature specific heat. It was also hoped that some information on electronic behavior in the normal and superconducting states might be obtained.

In the limit in which the number of degrees of freedom of the crystal becomes infinite, only negligible errors are introduced into the calculation of the frequency distribution function and the thermodynamic quantities by assuming cyclic boundary conditions. However, as the particle size decreases so that the ratio of the surface to volume becomes large, surface and size effects alter the thermodynamic functions and give rise to distinctly observable effects.

If the vibrational frequency spectrum of an isotropic elastic continuum with a surface can be approximated by two independent terms, one contributed by atoms on the surface with two-dimensional behavior and the other by the remaining atoms, one obtains at low temperatures in the Debye approximation a lattice specific heat consisting of a sum of surface- and bulk-phonon terms with T^2 and T^3 temperature dependences, respectively. In order to calculate the relative importance of the surface-phonon term, the vibrational frequencies for a crystal with a surface have to be determined. Several calculations which have been carried out for finite and semi-infinite isotropic elastic continua[1,2] and for a simple-lattice model[3] yield the lattice specific heat at low temperatures in the form

$$C_p = BST^2 + AVT^3 + \cdots , \tag{1}$$

where S and V are the surface area and volume of the crystal, respectively. The second term in (1) is the usual Debye volume term and the function B in the first term is

$$B = 3k_B^3\xi(3)\,(2v_t^4 - 3v_t^2v_l^2 + 3v_l^4)/4\pi\hbar^2v_t^2v_l^2(v_l^2 - v_t^2), \tag{2}$$

where v_t, v_l are the transverse and longitudinal sound velocities and $\xi(3)$ is a Riemann function, the other constants having the usual meaning. Reexamination of the lattice properties of small particles and films by numerical methods of lattice[4,5] and molecular dynamics[6] shows that the qualitative behavior of small particles may be different from the behavior of bulk crystals with surfaces. The specific heat of small particles does not take the form (1) and the vibrational heat capacity is not a monotonic function of the particle size.[5] These results are expected since there are only a finite number of vibrational modes in a small particle, whereas a semi-infinite crystal has a quasicontinuum of modes and also small particles have edges and corners as well as surfaces.

Comparison of the electronic properties of an assembly of small metal particles with those of bulk metal reveals significant differences. The electronic wave functions are subject to nonperiodic boundary conditions imposed by the particle surface and the energy spectrum becomes discrete in a system with small dimensions. Single-electron states must be consistent with charge conservation because of the large electrostatic energy required to add an elementary charge to the parti-

cle.[7] When the average separation between electronic levels is not small compared with the thermal energy k_BT, the small-particle specific heat differs from the bulk and its temperature dependence reflects the distribution of the energy levels.[8,9]

The thermodynamic properties of small particles or films have not been extensively investigated by specific-heat measurements. Heat capacities of NaCl[10] and MgO[11] powders revealed enhancements 2–4 times greater than predicted by semi-irfinite theories, but the results did not exhibit the extensive properties expected from these theories—the proportionality of the excess to the surface area and to T^2. Discrepancies were attributed mainly to the inaccuracies in surface-area determination. However, agreement with theoretical calculations[12] was obtained in the recent work of Barkman *et al.*[13] on NaCl with the experimental error ± 20% for the excess specific heat.

Specific-heat measurements on metallic particles, or on very small systems (< 100 Å) which are expected to show size effects, and a systematic investigation of properties for several surface areas have not been previously performed. Therefore we investigated the heat capacity of small particles of lead and indium from 1.5–15 K. The preliminary results of these measurements have already been reported.[14]

Section II of this paper is devoted to a description and characterization of the samples, to the experimental arrangements, and to tests of the accuracy of the specific-heat measurements. In Sec. III the results on bulk lead, 22-, 37-, 60-Å lead particles, and 22-Å indium particles are presented and the lattice behavior examined. In Sec. IV the size effects on the lattice specific heat are discussed. Section V deals with the observed electronic properties, changes in the electronic specific heats, and the effects on the superconducting transition temperatures.

II. EXPERIMENTAL

The systems studied in this work were small metal particles embedded in porous glass. The advantage of these systems over films is the increased amount of material. The glass samples are prepared by leaching a phase-separated alkali-borosilicate glass[15] to remove the boron-rich phase and leave the porous body. Typical porous glasses contain 96-wt% SiO_2, 3-wt% B_2O_3, and small amounts of Na_2O_3, Al_2O_3 and other oxides.

The samples were prepared by impregnating porous glass with metal. The glass samples were heated in a vacuum at temperatures up to 600 °C to remove adsorbed water vapor and gases, and then weighed and transferred in the protection of a dry box into a high-pressure chamber with metal of 99.9999% purity. The chamber was evacuated and heated above the melting point of the metal. The pressure required to fill the pores ranged from 0.8 to 6 kbar for pore diameters from 140 to 22 Å. After impregnation the samples were weighed again to determine the amount of metal left in the glass. The lead samples were stable at room temperature, but indium samples exhibited extrusion of the metal and had to be kept at nitrogen temperatures to preserve them. The average porosity of the glass varied from 15 to 25% and the filling coefficient ranged from 40 to 60%.

The pore size was found from adsorption and desorption isotherms of nitrogen at temperatures near its condensation point and by mercury porosimetry. In the first method the Kelvin equation[16] which relates the vapor pressure above a curved surface to its radius of curvature was used. It was assumed that the capillaries are circular in cross section. The evaporation pressure in the region of the steepest part of the desorption curve determines the pore diameter after allowing for the Brunauer–Emmett–Teller (BET) multilayer adsorption.[17] The second method[18] is based on measuring the volume of mercury which penetrates into the porous samples as a function of pressure, which is inversely proportional to the pore diameter. Typical porosimetry curves and size distribution curves for 60- and 37-Å samples are shown in Fig. 1. Considering the assumptions about the shapes of the pores, the properties of

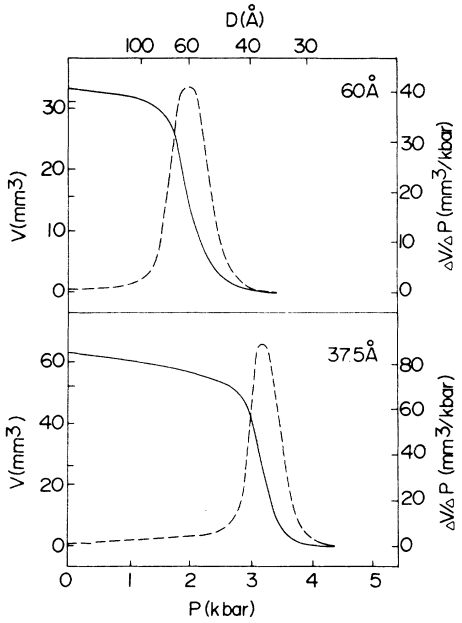

FIG. 1. Mercury porosimeter curves for the determination of pore size of glasses showing the dependence of volume filled (V) and size distribution curves ($\Delta V/\Delta P$) vs pressure P and diameter D represented by the solid and dashed curves, respectively.

the adsorbents, and the fact that the mercury porosimetry diameters correspond to the neck dimensions of the capillaries, the agreement within 10% between the two methods[19] seems to be satisfactory.

Provided that the porous structure was not destroyed during impregnation the size of the metal particles would correspond to the size of the pores. This was verified with the mercury porosimeter since the maxima of the size distribution curves dV/dP occurred at about the same pressure for two successive runs. Electron-transmission micrographs of metal in porous glass[20] showed that the metal forms a network of beads of uniform diameter, in close proximity, or in contact. The particle sizes determined from the micrographs agreed with the pore sizes of the glass.

Samples of metal-impregnated glass were examined by x-ray and neutron diffraction, which show that the grains retain the crystalline structure even at the smallest sizes.[21] The information about the crystallinity is important because the specific heats of amorphous solids are generally greater than the values of the heat capacities of crystalline solids of the same substance. These disorder enhancements of the lattice heat capacity would probably be more important than the lattice enhancements due to surface effects. X-ray diffraction patterns and elastic neutron scattering measurements at room temperature did not reveal strain on the metal from its surroundings. Moreover, neutron scattering measurements at nitrogen temperature revealed an increase of the average lattice constant of lead particles which is indicative of the lack of constraints on the atoms at the surface.[21] The x-ray and neutron lines broadenings are smaller than would be expected on the basis of size broadening using sizes determined by the above methods. This implies that the coherently scattering regions persist over distances of about 3 particle diameters. Therefore, the metal in glass can be described as a three-dimensional system of crystalline particles with diameters as determined by nitrogen adsorption, mercury porosimetry, and electron microscopy, but interconnected on the average over distances of several particle diameters. In addition, it was ascertained that the particles in the sample interior are not oxidized.

From the theoretical point of view the main objection common to most of the systems on which the heat capacity can be investigated is that the surfaces are not completely free. The surface-phonon behavior is altered by contact of the particles, films, or powders with the surroundings or with each other. It is clear that some "contact" between metal and glass must exist to support the particles and to provide a finite thermal conductivity between particles and the surroundings. However, the electron-microscope pictures show irregularities in the shape of the pores and metal particles which would limit the contact area to several spots on each particle. Differences in thermal contraction between glass and metal will cause the diameter of the metal particles to be reduced during cooling to low temperatures by 0.14–0.40 Å more than the diameter of 22–60-Å pores. The experimental room-temperature values of root-mean-square (rms) displacements of the surface atoms of lead are 0.26 Å as compared with the bulk value of 0.16 Å.[21,22] The rms displacements are reduced substantially on cooling to low temperatures (e.g., at nitrogen temperature the average rms displacement of atoms in 37-Å particles is 0.11 Å, while the bulk value is 0.087 Å[21]), and thus at low temperatures the sum of the rms displacements of glass and metal surface atoms is smaller than the increase of the average distance between equilibrium positions of glass and metal surface atoms even at contact spots. These estimates and experimental details indicate that a substantial part of the surface of the lead particles may be considered to be free at low temperatures. This conclusion seems also to be supported by the low thermal diffusivity of the samples which is of the same order as that of porous glasses although the glass-metal samples contain metallic regions of high thermal diffusivity.

The situation with indium particles which are unstable at room temperature and therefore in a state of unrelieved strain might be less favorable. The differential thermal contraction and reduction of rms displacements relieves the strain on cooling to low temperatures, but the indium particles might have only partially free surfaces.

Transition-temperature, critical-field, magnetization, and critical-current-density measurements on metals in porous glass were performed by Watson.[23] Pure bulk lead and indium are type-I superconductors; however, these systems are dirty type-II superconductors since the electronic mean free path becomes much smaller than the coherence length. The critical field increases by about a factor of 100 and is inversely proportional to the diameter of the particles. The magnetization curves show hysteretic behavior and the critical current densities reach 10^4–10^5 A/cm^2 in zero magnetic field at zero temperature.

Because the samples were small and had very low thermal diffusivity, the specific-heat measurements presented problems, particularly in minimizing heat leaks and thermal nonequilibrium in the calorimeter assembly. A detailed description of the experimental arrangements and the corrections for the heat leaks and nonequilibrium applied in the calculations of the specific heat are

given elsewhere,[24] and only a few features will be mentioned here.

The conventional discontinuous heating technique was chosen except for the investigation of the transition region, where continuous heating with low power input was employed to obtain a high density of data points. The low-heat-capacity calorimeter with a germanium thermometer and heater usually contained four samples prepared in separate runs; thus the average properties of the samples were investigated. Samples contained typically about 1–2 g of metal and 1–2 g of glass and had thermal conduction paths of 1.8 mm. The calorimeter was cooled and thermally isolated through a mechanical heat switch operated pneumatically to minimize the energy input on opening. The temperature of the isothermal shield was usually measured with another germanium thermometer and controlled in the middle of the intended temperature interval in order to reduce heat leaks.

The germanium temperature sensors were calibrated against He^4 vapor pressure below 4.2 K, and above this temperature against another germanium resistor standard. The thermometer and heater resistances were measured in four wire arrangements with dc potentiometers. Current through the resistors was supplied by constant-current sources. The time to reach thermal equilibrium in the after-heating period usually did not exceed 30 minutes. The corrections for heat leaks and thermal nonequilibrium were performed numerically.[24]

The random errors in the total heat capacity were estimated to be ± 1% and were primarily due to errors in the correction of temperature drifts and thermal nonequilibrium. Systematic errors were almost entirely due to the uncertainties in the temperature scale and thermometer calibration, and are estimated not to exceed 0.5%.

In order to test the general performance of the calorimetric system, the application of corrections, the temperature scales, and thermometry, the specific heat of copper was measured. The copper sample was deliberately connected by a weak thermal link to the calorimeter to simulate the poor thermal diffusivity of the glass-metal samples. The 0.2003-mole copper specimen was sample T4.5 from the 1965 Calorimetry Conference copper standard. The data from the entire temperature range, 1.5–15 K, were fitted by weighted least squares with a polynomial in odd powers of temperature,

$$C = \sum_{i=1}^{k} A_i T^{2i-1}. \tag{3}$$

Each measured point (T_i, C_i) was assigned a weight $\omega_i = (1/C_i)^2$ in the least-squares analysis so that fractional deviations from the curve were minimized. An adequate fit was obtained with $k = 4$, which yielded a percentage root-mean-square deviation of 0.5% and the coefficients A_i as follows:

$$A_1 = 0.69497,\ A_2 = 0.47521 \times 10^{-1},$$

$$A_3 = 0.23775 \times 10^{-5},\ A_4 = 0.61928 \times 10^{-7}.$$

When these coefficients are substituted into (3), the resultant specific heat has units mJ/mole K. These units will be used throughout the paper unless otherwise indicated. Comparison of this result with the copper reference equation[25] established as an average of measurements of different workers indicated an excellent agreement over the whole temperature range, with maximum deviations lower than 0.4% (see Fig. 2). Also the agreement of the electronic specific-heat coefficient $\gamma = 0.69497 \pm 0.004$ mJ/mole K^2 and the Debye temperature $\Theta(0) = 344.5 \pm 1.1$ K with those of the reference equation is very good. The error limits in the coefficients from our measurements are the sums of the estimated systematic errors and the 95% confidence limit from the statistical analysis.

III. LATTICE SPECIFIC HEAT

The specific heat of bulk lead was measured for the following reasons: Most of the measurements on small particles were intended to be performed with lead samples and a direct comparison between small-particle and bulk results was desirable to determine the enhancements without systematic errors. Moreover, it was appropriate to test the performance of the system in the region of the superconducting-to-normal transition and it was planned to cover the region 8–14 K which was not investigated in previous measurements. Finally it was hoped to resolve some disagree-

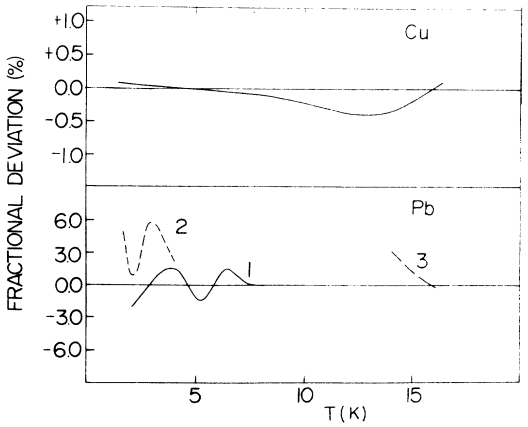

FIG. 2. Comparison of the specific heat of (a) copper with copper reference equation, Ref. 25, and (b) lead in the superconducting state and the normal state above transition temperature with (1) Ref. 26, (2) Ref. 27, and (3) Ref. 28.

TABLE I. Coefficients of least-squares polynomials (3) representing the specific heat in the superconducting state and in the normal state above T_c in (a) lead and (b) indium. C is given in mJ/mole K, PRMS and acc. stand for percentage root-mean-square deviation and accuracy of the measurement, respectively.

(a)

	C_s^B	C_s^{22}	C_s^{37}	C_s^{60}
A_1	0.3977652×10^{0}	-0.226489×10^{0}	-0.385105×10^{1}	-0.135546×10^{1}
A_2	0.1218511×10^{1}	0.246742×10^{1}	0.498437×10^{1}	0.275238×10^{1}
A_3	0.1851371×10^{0}	0.123412×10^{0}	-0.415926×10^{0}	-0.668200×10^{-1}
A_4	-0.2262992×10^{-1}	-0.118079×10^{-1}	0.327207×10^{-1}	0.854007×10^{-2}
A_5	0.1532147×10^{-2}	0.635659×10^{-3}	-0.113528×10^{-2}	-0.334514×10^{-3}
A_6	-0.5014263×10^{-4}	-0.150325×10^{-4}	0.185042×10^{-4}	0.588362×10^{-5}
A_7	0.7775348×10^{-6}	0.126017×10^{-6}	-0.116755×10^{-6}	-0.396876×10^{-7}
A_8	-0.4605184×10^{-8}			
PRMS(%)	0.5	1.1	1.9	0.9
Acc. (%)	±1	±2	±3	±2

above T_c

	C_n^B	C_n^{22}	C_n^{37}	C_n^{60}
A_1	0.1702586×10^{3}	-0.875303×10^{2}	-0.146366×10^{3}	-0.118224×10^{3}
A_2	-0.1084259×10^{2}	0.690325×10^{1}	0.916446×10^{1}	0.766827×10^{1}
A_3	0.4075688×10^{0}	-0.385481×10^{-1}	-0.759271×10^{-1}	-0.531514×10^{-1}
A_4	-0.5908675×10^{-2}	0.120472×10^{-3}	0.359124×10^{-3}	0.226229×10^{-3}
A_5	0.4713268×10^{-4}	-0.152112×10^{-6}	-0.768743×10^{-6}	-0.465779×10^{-6}
A_6	-0.2146553×10^{-6}	0.733737×10^{-11}	0.494757×10^{-9}	0.312224×10^{-9}
A_7	0.5223596×10^{-9}			
A_8	-0.5266274×10^{-12}			
PRMS(%)	0.3	0.6	1.0	0.4
Acc. (%)	±1	±2	±3	±2

(b)

	C_s^B (Ref. 38)	C_s^{22}	C_n^B (Ref. 38)	C_n^{22} above T_c
A_1	-0.55901×10^{0}	-0.6553×10^{1}	-0.1725185×10^{1}	-0.164514×10^{2}
A_2	0.22066×10^{1}	0.7307×10^{1}	0.1662915×10^{1}	0.540944×10^{1}
A_3	0.51218×10^{-1}	-0.8236×10^{0}	0.1528370×10^{-1}	-0.105525×10^{0}
A_4	-0.28572×10^{-1}	0.7815×10^{-1}	-0.2489305×10^{-3}	0.191035×10^{-2}
A_5	0.35824×10^{-2}	-0.3483×10^{-2}	0.1487103×10^{-5}	-0.203223×10^{-4}
A_6	-0.14125×10^{-3}	0.5898×10^{-4}	-0.4582531×10^{-8}	0.117845×10^{-6}
A_7			0.7207751×10^{-11}	-0.346614×10^{-9}
A_8			-0.4575364×10^{-14}	0.404869×10^{-12}
PRMS(%)		1.1		0.8
Acc. (%)		±2		+2

ments (up to 6%) in the previous results in the superconducting state.[26,27] Below T_c the specific heat in only the superconducting state was investigated.

The measurements were performed on a 0.0881-mole sample cast of 99.9999%-pure lead. The results were represented with polynomials (2) separately in the superconducting and normal region, the coefficients A_i being given in Table I. The values of the specific heat obtained by evaluating the polynomials are presented in Table II. In the overlapping temperature region from 2 to 8 K our results are in good agreement with the values determined by Neighbor *et al.*[26] (deviations shown in Fig. 2), but there is a discrepancy of up to 6% with the measurement of van der Hoeven and Keesom[27] around 3 K. Comparison with another set of data above 14 K[28] also shows good agreement.

The specific heat of small metal particles measured from 1.5–15 K was evaluated by subtraction of the heat capacity of addenda, which included the calorimeter and glass contributions. These were determined in separate measurements and accounted for 40–50% of the total heat capacity, with the glass and calorimeter contributing roughly the same amount. Enhancements in the specific heat of porous glasses above the values for solid glass were also observed.[14,40] These excesses (< 60% of the solid glass value) probably arise from surface-phonon modes present in the empty porous glass. The contact between the walls of the glass pores and the metal will reduce the free-surface area of the glass and decrease its specific

TABLE II. Table of specific-heat values (in mJ/mole K) for bulk and small particles of lead and indium in the superconducting state and in the normal state above T_c.

T (K)	Pb				In	
	C^B	C^{22}	C^{37}	C^{60}	C^B	C^{22}
1.5	5.783	8.75	8.40	6.88	6.635	9.78
1.75	9.341	14.4	14.6	11.7	10.74	17.6
2.00	14.26	22.0	22.5	18.1	16.06	27.3
2.25	20.76	32.1	32.1	26.5	22.73	39.1
2.50	29.06	44.9	43.7	37.2	30.94	53.2
2.75	39.39	60.8	57.6	50.5	41.04	70.0
3.00	52.04	80.2	74.3	67.1	S53.35	90.3
3.50	86.15	131	119	112	N71.80	143
4.00	137.0	202	186	177	111.5	S213
4.50	212.2	300	280	265	163.7	N282
5.00	317.6	432	404	381	230.2	379
6.00	609.1	S784	S726	703	411.4	618
7.00	S1046	N1200	N1110	S1130	661.8	921
8.00	N1525	1800	1690	N1650	980.4	1290
10.00	2894	3230	2980	3000	1781	2200
12.00	4484	4820	4460	4540	2705	3200
15.00	7135	7510	7160	7190	4216	5060

heat. However, this will not significantly affect the metal results, because the contribution of glass to the total heat capacity is small (e.g., if the total free surface of glass is decreased by 10%, the maximum decrease in the total heat capacity is less than 1%).

Measurements were performed on 22-, 37-, 60-Å lead and 22-Å indium particles and the specific-heat results for 60-Å lead and 22-Å indium particles are shown in Figs. 3 and 4, respectively. Below T_c the specific heat in the normal state was not measured because the magnetic fields required to drive the small particles normal are of the order of $10T$. The results were fitted with odd-power polynomials (2) in the superconducting and normal regions; adequate fits over the whole temperature range required polynomials of order 5–8 and no physical meanings are ascribed to the coefficients in this case. However, it was possible to represent the results well in a limited region, say 1.5–3 K, with two-term polynomials. The random errors in the total heat capacity were typically ± 1%; after subtraction of the addenda heat capacity the precision of the small-particle results was about ± 2%, as shown in Fig. 5. The coefficients of the polynomials and the tabulated specific-heat results are given in Tables I and II, respectively.

In all cases substantial enhancements in the specific heat were observed, ranging from 75% of the bulk value around 2 K to a few percent at 15 K. The enhancements are simply defined as the difference between the heat capacity of the small particles and that of bulk. However, in metals both lattice vibrations and electrons contribute to the specific heat and the computed enhancements will correspond to changes in phonon and electronic behavior. For a complete analysis of the results the measurements in the normal state below the transition temperature would be required, and even in that case the separation would not necessarily be clear since the lattice specific heat of the particles does not have a simple temperature dependence and the electronic part can be nonlinear.[8,9]

In bulk lead, the electronic superconducting specific heat contributes from 1.5 K to T_c from 2 to 7% of the total. Furthermore, the transition temperatures of small lead particles are not very different from the bulk transition temperature. In a first approximation we can neglect changes in the electronic behavior and the excess specific heat will correspond to the phonon enhancements alone. Surface atoms are bound by weaker forces because of missing neighbors, which leads to lower characteristic frequencies and large displacements for these atoms compared with interior atoms. The downward shift of frequencies of atoms at or near the surface and an attendant

TABLE III. Average values of the transverse and longitudinal sound velocities and the lattice enhancement constant B.

Element	$\bar{V}_t$ (10^{-5} cm/sec)	$\bar{V}_l$	$B(0)$ (10^8 mJ/K^3 cm^2 mole)
Pb	0.96	2.38	2.21
In	0.97	2.73	2.19

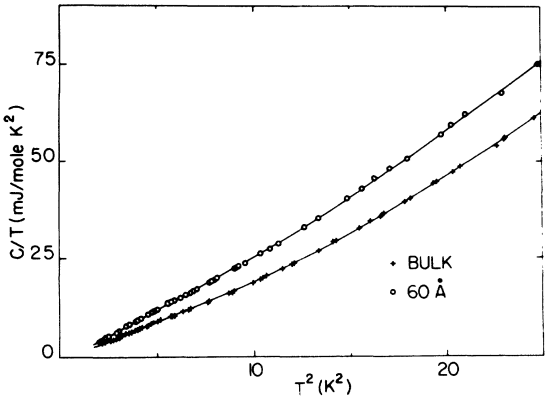

FIG. 3. Specific heat of bulk lead and 60-Å lead particles in the superconducting state below 5 K.

depletion of the higher-frequency lattice vibrations results in enhancements of the lattice specific heat. The experimental enhancements are plotted vs T^2 in Fig. 6 together with the theoretical predictions from theories for semi-infinite crystals.[2,3] The theoretical curves were calculated with the assumption that the particles are long cylinders and their surfaces are totally free. When a metal is approximated by separated spheres, as was done in previous publications,[14] the total free surface increases up to 50%. The actual free-surface area will be between these two limits, probably closer to the former.

Since the theoretical results are derived for isotropic solids, the function B in (2) involving the sound velocities has to be averaged over all directions of propagation. Average speeds of sound $\bar{v}_i$ are determined from

$$\bar{v}_i^{-3} = \int \frac{d\Omega}{4\pi v_i^3} , \quad i = 1, 2, 3 \tag{4}$$

where $d\Omega$ is an element of solid angle. For any particular direction the integrand in (4) is found by solving the equation of motion for elastic waves using the elastic constants for lead[29] and indium.[30] The transverse velocity $\bar{v}_t$ taken as an average of the two transverse $\bar{v}_i$ from (4) and the longitudinal velocity $\bar{v}_l$ are given in Table III together with the enhancement factor $B(0)$, which is approximately constant at low temperatures.

Considering the limits of accuracy of our estimate for the free-surface area of particles, good agreement is found between theoretical and experimental magnitudes of the excess specific heats above about 4 K with the exception of 22-Å lead particles. Serious qualitative discrepancies arise both in the temperature dependence of the excess specific heat, which is not simply T^2 even over a limited temperature range, and also in the lack of proportionality to the surface area; these appeared in all small-particle measurements.

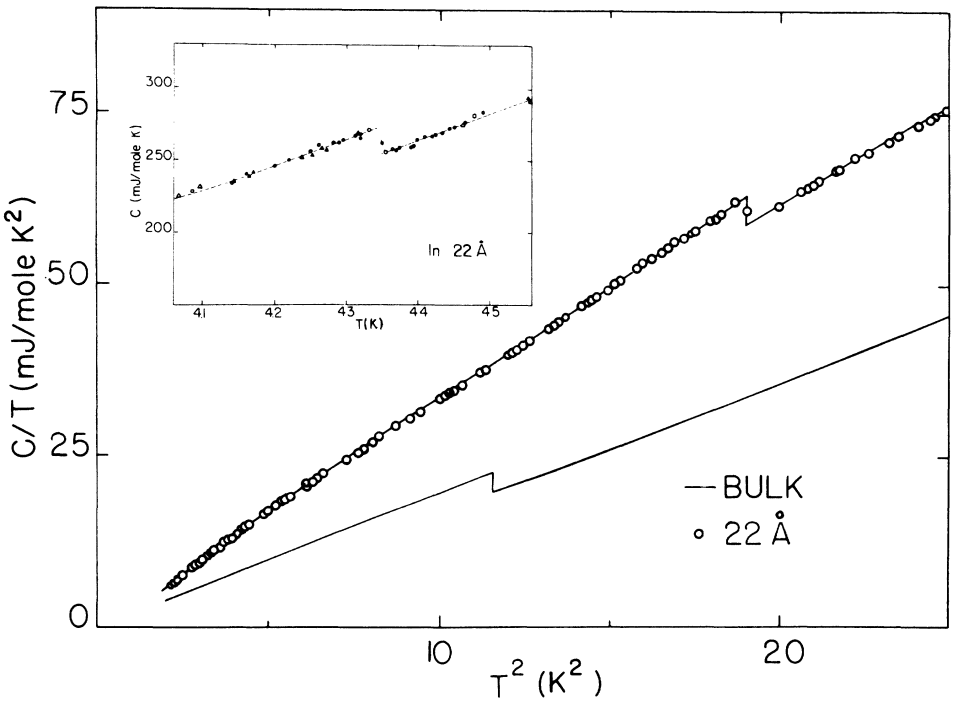

FIG. 4. The specific heat of 22-Å indium particles from 1.5 to 5 K plotted as C/T vs T^2. The insert shows the details of the transition region with continuous-heating data points taken as the average of eight experimental points. The solid curve indicates the bulk-indium specific heat, Ref. 38.

Reasons for these discrepancies may lie in the nonideality of the epxerimental systems or in the inadequacies of the semi-infinite theories. In the first case an immediate question arises with respect to the effect of some "contact" between the metal and the surroundings. As indicated above the surfaces are probably essentially free at low temperatures, but contact can effectively decrease the magnitude of the surface heat capacity and in special circumstances its proportionality to the surface area. If the number of contacts per unit area of surface is the same for small and large particles, the proportionality should not be affected. The temperature dependence of the surface specific heat is probably not altered by contact since for surfaces which are completely free, one would expect from the semi-infinite theories enhancements proportional to T^2, whereas in the extreme opposite case of a solid with completely clamped surfaces, it is predicted that a T^2-dependent decrease should be observed. This negative contribution in the latter case arises from imposing additional restraints on the vibrating system which raise the phonon frequencies and lower the specific heat. Thus it seems that the discrepancies cannot be attributed to the nonideality of the experimental system, and therefore the applicability of theoretical calculations was examined.

The continuum models are valid only at low temperatures, where the dispersion of the modes is unimportant, typically at temperatures below $\Theta/30$. The semi-infinite calculations may not be applicable to small particles since their vibrational spectrum can be completely different from that of semi-infinite crystals. According to one theoretical estimate[3] the difference in the excess specific heat should be less than 10% for indium or lead if

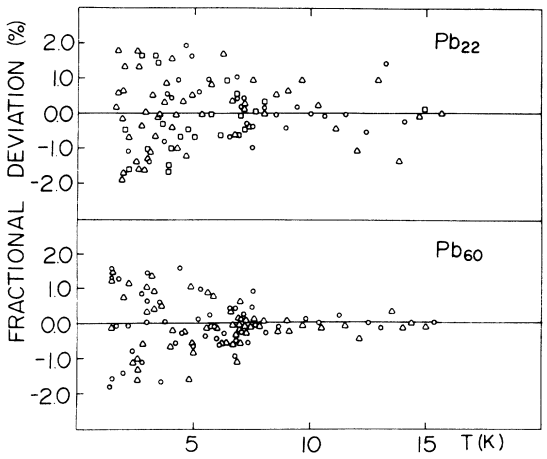

FIG. 5. Fractional deviations of the specific-heat data points from the fitted polynomials (3) for 22- and 60-Å lead particles.

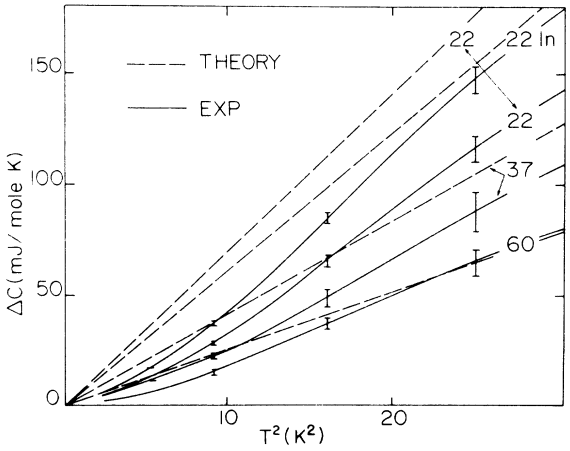

FIG. 6. Enhancements in the specific heat of small lead (22, 37 and 60 Å) and 22-Å indium particles above the bulk values and the predictions of the semi-infinite theories.

$dT \gtrsim 3\times10^{-9}$ mK, where d is the diameter of the particle and T is the temperature, so that for 22-Å particles the difference should be less than 10% above 1.5 K. However, we believe for the following reasons that this seriously underestimates the difference. The stress-free surfaces assumed in the calculations are more realistic boundary conditions than models with perfectly reflecting faces used previously, but even these might be an inadequate description of the real free surface. The calculations neglect changes of the force constants of atoms near and at the surface, which can amount to a large decrease of the nearest-neighbor force constants by relaxation[31] and result in the corresponding decrease of the higher frequencies for surface modes.[4] Relaxation effects are important for the specific heat at intermediate temperatures, but do not effect it at very low temperatures for the semi-infinite solids, because the lowest-frequency surface modes contributing significantly to the surface specific heat penetrate deeply into the solid and are thus insensitive to what happens at the surface. However, the relaxation effects might be more important in small particles because these longest-wavelength phonons are cut off by the particle size. Size quantization in small particles can result in a discrete phonon spectrum and hence a low-frequency cutoff, which may give significant effects at temperatures where the Debye-like behavior occurs; this aspect will be discussed in Sec. IV.

Recently it was reported that no enhancements above the bulk specific heats were observed in indium and lead films.[32] In view of our results it is easy to ascertain that the expected enhancements are lower than the accuracy of these measurements. Large increases in the lattice heat capacity of

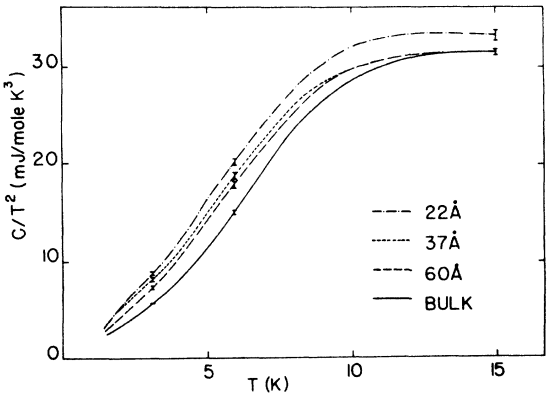

FIG. 7. Lattice specific heat of bulk lead and small lead particles plotted as C/T^2 vs T. Deviations in the transition region are smeared out.

granular aluminum films have been detected,[33] but the presence of oxides on the grain surfaces and large grain inhomogeneities do not permit one to relate the excesses to surface effects. Moreover, the heat-capacity contribution of the inert gas trapped in the films could account for the observed increases.

IV. SIZE EFFECT ON PHONONS

The quantum size effect may be defined as the dependence of the properties of solids on their characteristic dimensions, when the latter become comparable with the effective wavelength of the elementary excitations. It is proposed here that the observed effects are consistent with the effect of finite size on the phonon spectrum. Low-frequency phonon modes contribute most to the low-temperature specific heat and thus removal of part of these frequencies would cause a rapid decrease of the specific heat at the lowest temperatures. It is observed that below 2.5 K the heat capacities of the 22- and 37-Å lead particles agree within experimental accuracy. The indications that the quantum size effect is involved may be illustrated on two graphs. If one assumes that the specific heat can be separated into two parts arising from volume and surface contributions, that the surface part has a temperature dependence of the form T^{α}, and that the volume part is unchanged in magnitude and temperature dependence, one should obtain by plotting C/T^{α} vs T curves shifted above the curve representing the specific heat of the bulk metal by an amount independent of temperature and proportional to the surface area. As can be seen in Fig. 7, the curves for small particles for $\alpha = 2$ are shifted by approximately constant values above the bulk curve below 8 K except at the lowest temperatures, where they start to fall off. The simple power-law temperature dependence of the surface enhancement term is expected only at temperatures much lower than the Debye temperature, as remarked earlier. Also, since the predicted temperature dependence of the surface enhancement ΔC is of lower order than that of the bulk-phonon specific heat C_p^B, and if no other effects were present, the ratio $\Delta C/C_p^B$ should be an increasing function with decreasing temperature. It can be noticed in Fig. 8 that the ratios start to fall off near 4 K and at the lowest temperature the ratios decrease with lowering of the temperature. For comparison, the solid line calculated from the excess specific heat between 5 and 6 K shows the expected behavior of the enhancements if they were T^2 dependent.

The smallest wave vector q allowed in a particle with characteristic dimension d is of order $q = \pi/d$, and in the isotropic-continuum approximation the corresponding cut off temperature is

$$\Theta_C = \hbar\omega q/k_B . \tag{5}$$

The complicated geometry of the particles does not permit one to obtain definite quantitative values of Θ_C and falloffs. The cutoff temperatures Θ_{CS} and Θ_{CV} for the surface and volume modes, respectively, were evaluated for a vibrating sphere and a cylinder from relation (5), with the lowest wave vectors allowed in the vibrating system determined by solving the differential wave equations.[34] In Table IV these estimates of the cutoff temperatures Θ_C for the volume and surface modes for a sphere and a cylinder are summarized in columns 3–7.

The decreases in the specific heat due to low-temperature cutoffs Θ_{CV} and Θ_{CS} can be evaluated for an isotropic elastic continuum in the Debye ap-

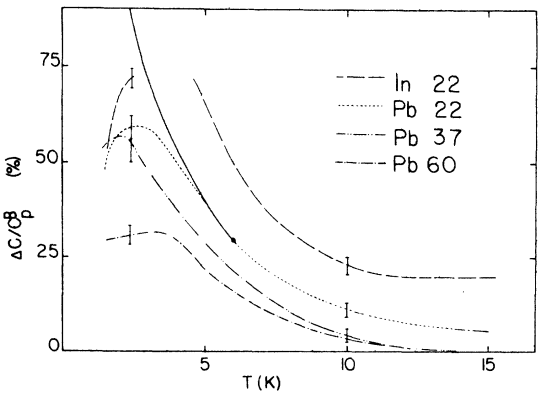

FIG. 8. Enhancements of the specific heat of small particles of indium and lead, ΔC, divided by the lattice specific heat of bulk indium and lead, C_p^B, respectively. The solid line indicates the ratio $\Delta C/C_p^B$ if the enhancements ΔC were proportional to BST^2. The value of BS is based on the enhancement at 6 K. Deviations near the transition for lead particles are smeared out and the region below T_c for indium particles is deleted.

TABLE IV. Theoretical and experimentally determined estimates of volume and surface size cutoff temperatures (in K).

Element	Diameter (Å)	$\Theta_C = h\pi\bar{v}_t/k_B d$	Θ_{CV} sphere	Θ_{CS} sphere	Θ_{CV} cyl. $l=3d$	Θ_{CS} cyl. $l=3d$	$\Theta_{CV}^{\text{expt.}}$	$\Theta_{CS}^{\text{expt.}}$
Pb	22	10.5	17.6	8.0	5.8	3.5	8.0	5.0
	37	6.1	10.3	4.7	3.4	2.1	5.5	3.1
	60	3.8	6.4	2.9	2.1	1.3	4.5	2.4
In	22	10.6	17.7	8.1	5.9	3.6	~8.0	~5.0

proximation by differences in integrals of the type

$$\int_0^{x_V} y_4(x)\,dx - \int_{x_{CV}}^{x_{V1}} y_4(x)\,dx$$

and

$$\int_0^{x_S} y_3(x)\,dx - \int_{x_{CS}}^{x_{S1}} y_3(x)\,dx \qquad (6)$$

for the volume and surface specific heats, respectively, where

$$y_\eta(x) = x^\eta e^x/(e^x-1)^2, \quad \eta = 4, 3$$

$$x = \hbar\omega/k_B T, \qquad x_i = \Theta_i/T,$$

$i = V, S, V1, S1$ labeling high-temperature cutoffs. The upper limits x_{V1} and x_{S1}, redefined so that the number of modes remains unchanged, can be set to infinity together with x_V and x_S at temperatures $T \ll \Theta_V, \Theta_S$. The procedure can also be used to assign cutoffs to known decreases with the help of the tabulated values of the integrals (6).[35]

Experimental decreases of the specific heat were determined as the difference between the measured values and the values expected if the size effect were not present. The latter were estimated from an extrapolation to low temperatures of the C/T^2-vs-T plot in 5–8 K range. If the relative importance of the surface and volume terms for the decrease at any temperature is assumed to be given by the ratio of their contributions to the total specific heat, the experimental decreases can be accounted for with average cutoff temperatures listed in the last two columns of Table IV.

The experimental cutoff temperatures in every case lie within the theoretical limits set for a sphere and a cylinder, which can be considered to be a reasonable agreement in view of the many oversimplifications of the model. The size quantization will change the phonon quasicontinuum into a spectrum of discrete frequencies, so that the estimates based on the integrations with the cutoff temperatures as lower limits will yield completely incorrect results and summations should be used instead. Furthermore, the relative importance of the surface and volume terms in the decrease may be different from the assumed one, and the frequency spectrum of the particles is not necessarily given by a sum of the linear and quadratic terms in the wave vector.

"Contact" of the grains with the medium could enable the propagation of some low-frequency modes from the surroundings into particles. This effect would effectively lower the cutoff temperatures. On the other hand the size effect may play a role at higher temperatures (above 5 K), where it was *a priori* assumed for the evaluation of experimental cutoffs that they are not involved. The theoretical cutoffs shown in Table IV are only lower limits of a series of cutoff values and these may decrease the heat capacity in the whole measured range. Finally it should be pointed out that for very small particles it might not be appropriate to differentiate between contributions of surface- and volume-phonon modes to the specific heat.

Another interesting aspect of the data is the existence of maxima in the surface specific heat ΔC of lead particles (see Fig. 9; the anomalous behavior near the superconducting transition temperature will be discussed later). These maxima occur roughly at $T \simeq 0.1\,\Theta_V$, a temperature corresponding to energies at which the density of surface-phonon states is high. Similar behavior was observed[13] and theoretically accounted for with numerical lattice dynamical calculations for NaCl.[12]

The magnitude of the ΔC peaks are 10 ± 3, 8.6 ± 2, and 10 ± 2.5 μJ/K m^2 for 22-, 37-, and 60-Å lead particles, respectively, if a cylindrical shape for the particles is assumed in the estimate of the surface area. The measurements have not been carried out above 15 K because the enhancements at these temperatures are rather low and hence the inaccuracy in the surface specific heat is large. Consequently the variation of the positions and the magnitude of the maxima as a function of particle size might not be significant. The maximum in the surface specific heat of indium probably appears above 15 K and the peak magnitude is greater than 31 ± 4 μJ/K m^2. The occurrence of a maximum in indium particles at higher temperatures compared with lead is expected since a high density of surface-phonon states in indium will appear at higher energies. This is due to the fact that the maxima of the bulk-phonon density of states of indium lie at higher energies than those of bulk lead.

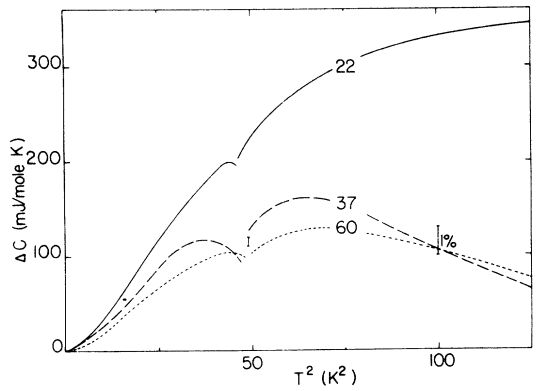

FIG. 9. Enhancements in the specific heat of small lead particles above the bulk value plotted as $\Delta C = C^{SP}_{s,n} - C^{B}_{s,n}$ vs T^2. The region near the superconducting transition is deleted. The plot indicates the possible decreases in the electronic specific heat in the superconducting state.

The occurrence of maxima in the enhancements can be easily understood by considering the behavior in the limits of low and high temperature. Low-temperature lattice properties of small particles are governed by the finite-size effect, which results in a faster decrease of their vibrational heat capacity when the temperature is lowered as compared to the infinite crystal, both approaching zero as the temperature goes to zero. At high temperatures each mode of vibration contributes the classical amount k_B to both small particle or bulk specific heats, and since the total number of modes is unchanged the surface enhancements have to approach zero. Therefore the presence of the surface modes is reflected by a maximum in the surface specific heat at intermediate temperatures.

V. ELECTRONIC PROPERTIES AND TRANSITION TEMPERATURES

The usual heat capacity analysis into lattice (p) and electronic (e) contributions in the normal (n) and superconducting (s) state

$$C_n = C_{pn} + C_{en}, \quad C_s = C_{ps} + C_{es}$$

with

$$C_{pn} = C_{ps} \tag{7}$$

is adopted here for both small particles (SP) and bulk (B). C_{es} is determined as

$$C_{es} = C_s - C_n + C_{en} = \delta C + C_{en}. \tag{8}$$

For the bulk samples $C^{B}_{en} = \gamma T$, but C^{SP}_{en} cannot be determined since normal-state measurements below the transition temperature T_c were not performed and extrapolation to low temperature from above T_c could not be employed because of the high values of T_c.

Most of the information was acquired near T_c by the continuous-heating method. Low power input was used to prevent excessive temperature gradients in samples of low thermal diffusivity which could smear out the discontinuity δC at T_c. The steady temperature difference across the sample established on heating is proportional to the power input.[24] The temperature nonequilibrium was directly determined during discontinuous heating and this permitted an evaluation of the upper limit of power, which could be employed without setting up gradients greater than the width of the bulk-lead discontinuity.

The transition region results for 22-, 37-, 60-Å particles and bulk lead are shown in Fig. 10 and for 22-Å indium particles in Fig. 4. The transition temperatures listed in Table V agree with the value of T^{B}_{c} determined with an acoustic thermometer for bulk lead[36] and with T^{SP}_{c}'s detected by a mutual-inductance technique.[23] Our bulk-lead discontinuity $\delta C^{B}(T^{B}_{c}) = 58.0 \pm 1.5$ mJ/mole K is in agreement with a previous determination of 58.5 ± 0.9[26] and a magnetic result of 58.1 ± 0.7 mJ/mole K.[37]

A striking difference exists in the discontinuities of small lead and indium particles, the former being broad whereas the latter is quite sharp. The smearing may be due either to thermodynamic fluctuations or to a variation of T_c with particle size. When the dimensions of the small particles are much less than the coherence length ξ, fluctuations of the order parameter become important. However, if interparticle distances are small so that the particles are phase coupled by Josephson tunneling, the effective size of the superconductor can be greater than ξ, although the particle size d is less than ξ. Thus the system might exhibit three-dimensional behavior and the importance of the fluctuations can be suppressed, this hypo-

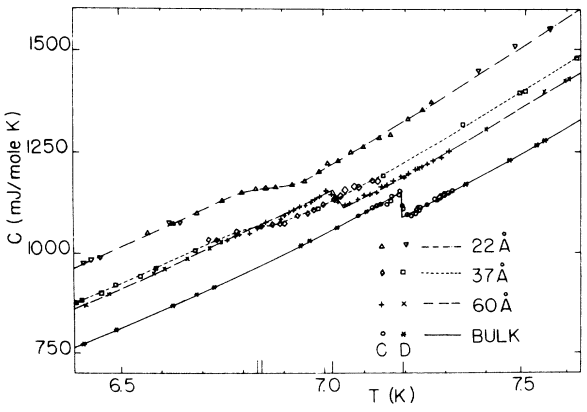

FIG. 10. Specific heat of bulk lead and small lead particles near the superconducting transition temperature. Continuous-heating data points (C) are averages of eight points taken with 10-mK temperature increments.

TABLE V. Superconducting transition temperatures T_c determined from the specific-heat measurements.

Sample	Pb^B	Pb^{140}	Pb^{60}	Pb^{37}	Pb^{22}	In^{22}
T_c (K)	7.209 ± 0.01	7.19 ± 0.01	7.04 ± 0.01	6.86 ± 0.05	6.83 ± 0.07	4.34 ± 0.01

thesis being supported by the absence of appreciable rounding of the indium discontinuity.

The dependence of T_c on particle size, a mechanism for which will be discussed later, can also round the discontinuity. Typically about 90% of the pores lie within 25% of a mean diameter and thus the size distribution results in a smearing of ±80, ±70, ±37 mK for 22-, 37-, and 60-Å lead particles, respectively (as estimated from the observed T_c-vs-$1/d$ dependence) and accounts for the observed broadening. The smearing of the discontinuity by a size distribution is small in 22-Å indium because $\delta T_c/\delta(1/d) \simeq 0$ around 20 Å.[23]

Using Eq. (7) we should find smooth curves for the lattice specific heats including enhancements. However, when the enhancements $\Delta C_{n,s} = C^{SP}_{n,s} - C^B_{n,s}$ are plotted vs temperature (Fig. 9) for lead particles, the depression of ΔC can be observed approximately from 5 to 8 K, excluding the data near T_c. These systematic deviations are attributed to decreases in C^{SP}_{es} and C^{SP}_{en} of lead particles with respect to the bulk value. In absolute terms the changes are very small (1–2% of C^{SP}) but they represent lowering of up to 30% of C^B_{es} and C^B_{en}. At lower temperatures the changes in C^{SP}_{es} cannot be resolved, because C^{SP}_{es} is less than 2% of C^{SP}_s. In the calculation of ΔC_s, the corrections for the depressed values of T^{SP}_c, which are likely to enhance the anomalous behavior, should be included, but they are uncertain. These decreases in C^{SP}_{es} and C^{SP}_{en} can be due to a decrease in the electronic density of states at the Fermi surface $N(0)$. However, it is necessary to emphasize that the observed changes in lead C^{SP}_{es} and C^{SP}_{en} are of the same order as the accuracy of the measurements, and hence the results and their interpretation should be treated with extreme caution.

The analysis of the electronic properties of indium particles is complicated because of the substantial enhancement of the transition temperature, so that only the behavior at T_c will be considered. The bulk discontinuity $\delta C^B(T^B_c = 3.4\ \text{K}) = 9.2 \pm 0.5$[38] should be compared with $\delta C^{22}(T^{22}_c = 4.34\ \text{K}) = 19.1 \pm 1$ for indium particles. Using $\gamma = 1.7$ mJ/mole K^2 (Ref. 38) and Eq. (8) we find $C^B_{es}(T^B_c) = 14.9$ mJ/mole K, whereas $C^{22}_{es}(T^{22}_c) = 26.4$ mJ/mole K with C^B_{en} used instead of the appropriate C^{22}_{en}. Even if C^{22}_{en} is completely neglected in (8), $C^{22}_{es}(T^{22}_c)$ is greater than $C^B_{es}(T^B_c)$. The ratios $\delta C(T_c)/\gamma T_c$ are approximately 1.6 and 2.6 for bulk and 22-Å indium, respectively. These interesting features imply that C^{SP}_{es} of indium is enhanced contrary to the behavior of superconducting lead particles. The increase in both T_c and C^{SP}_{es} may indicate an increase of the energy gap and the electron-phonon coupling constant (due to the softening of phonon spectrum), which appears as a move to a more strongly coupled superconductor as the particle size is decreased.

Anomalous behavior of C^B_p in indium has been reported and interpreted as a decrease of C^B_p accompanying the normal-superconducting transition.[38] This interpretation causes a substantial change of C^B_{es}, but is not supported by elastic constant measurements.[30] The inferred changes be-

TABLE VI. Tabulation of moments $\langle\omega^k\rangle$ determined with α^2F from electron tunneling, predictions of T_c's in small particles, the experimental Debye temperatures Θ, and experimental T_c/T^B_c.

	α^2F from tunneling							experimental results				
	$\langle\omega\rangle$ (meV)	$\frac{\langle\omega\rangle}{\langle\omega\rangle^B}$	$\langle\omega^2\rangle$ (meV^2)	$\frac{\langle\omega^2\rangle^B}{\langle\omega^2\rangle}$	λ	T_c (K)	$\frac{T_c}{T^B_c}$	Θ(4 K) (K)	$\Theta(T^B_c)$ (K)	$\frac{\Theta(4)}{\Theta^B(4)}$	$\frac{\Theta(T^B_c)}{\Theta_B(T^B_c)}$	$\frac{T_c}{T^B_c}$
Pb^B	5.2	1	31	1	1.50	6.28	1	99	88.4	1	1	1
Pb^{60}	4.94	0.95	28.3	1.095	1.64	6.53	1.04	90.8	85.2	0.92	0.96	0.98
Pb^{37}	4.77	0.92	26.5	1.17	1.755	6.69	1.065	89	84.4	0.90	0.955	0.95
Pb^{22}	4.57	0.88	24.4	1.27	1.905	6.86	1.09	86	82	0.87	0.93	0.945
In^B	6.90	1	61.0	1	0.83	3.42	1	106.2	107.4	1	1	1
In^{22}	6.07	0.88	47.9	1.27	1.06	4.77	1.39	86.2	86	0.81	0.80	1.29

Parameters used

Pb^B: $\mu^* = 0.13$; $\lambda = 1.5$; α^2F, Ref. 41 In^B: $\mu^* = 0.125$; $\lambda = 0.83$; α^2F, Ref. 42

tween C_{pn}^{B} and C_{ps}^{B}, if correct, would invalidate the previous analysis for indium. With the same percentage change in C_{ps}^{SP} as in C_{ps}^{B} the effect would tend to lower δC^{SP} even more than δC^{B} and thus would be a contradiction to the observed enhanced discontinuity. If a parallel between the bulk and the small-particle lattice behavior can be drawn, the interpretation of the bulk-indium result would not be supported by this measurement.

It is generally observed that the superconducting transition temperatures of films and small particles are enhanced. Numerous models have been proposed to explain enhanced T_c's and the most successful calculations demonstrate the dependence of T_c on changes in the phonon spectrum, [39] yielding the expression

$$T_c = \frac{\langle\omega\rangle}{1.2} \exp\left(-\frac{1.04(1+\lambda)}{\lambda-\mu^*(1+0.62\lambda)}\right), \tag{9}$$

where λ is the electron-phonon coupling constant, μ^* is the Coulomb pseudopotential,

$$\langle\omega^k\rangle = \int_0^{\omega_0} d\omega\, \alpha^2(\omega)F(\omega)\,\omega^{k-1} \Big/ \int_0^{\omega_0} d\omega\, \alpha^2(\omega)F(\omega)\,\omega^{-1}. \tag{10}$$

$F(\omega)$ stands for the phonon density of states, $\alpha^2(\omega)$ is the average of the electron-phonon interaction, and ω_0 is the maximum phonon frequency. For polyvalent metals one finds $\lambda \simeq N(0)\langle\tau^2\rangle/M\langle\omega^2\rangle$, where $\langle\tau^2\rangle$ is the average of the square of the electron-phonon matrix, and M the ionic mass. If the $N(0)$, $\langle\tau^2\rangle$, and μ^* of small particles are unchanged as compared with the bulk, the presence of additional low-frequency surface phonons and the attendant depletion of higher modes decreases $\langle\omega^2\rangle$ and thus usually enhances T_c.

The low-temperature specific heat does not provide sufficient information to predict changes of T_c from (9) in films or small systems, since $\langle\omega^2\rangle$ is not determined and the experimental $\langle\omega\rangle$ corresponds only to the average over the low-frequency part of the phonon spectrum. In order to estimate the moments $\langle\omega\rangle$ and $\langle\omega^2\rangle$ for small particles over the phonon spectrum a simple approximate scheme, described in detail elsewhere, [40] is adopted. The vibrational frequencies ω_i of any atom in the particle are obtained by scaling the bulk frequencies ω according to the atom's number of nearest neighbors n_i, that is, $\omega_i = (n_i/n)^{1/2}\omega$, where n is the number of nearest neighbors in the bulk. Then the fraction of atoms b_i in a given environment (with the same number of neighbors) is determined. The α^2F value for a given bulk frequency is divided into portions determined by the above fractions b_i. These portions are shifted to the renormalized frequencies ω_i, an approximate α^2F for small particles is generated, and moments (10) for the small particles are then given by

$$\langle\omega^k\rangle = \sum_i b_i \int_0^{\omega_{0i}} d\omega\, \alpha^2(\omega)F(\omega)\,\omega_i^{k-1} \Big/ \sum_i b_i \int_0^{\omega_{0i}} d\omega \times \alpha^2(\omega)F(\omega)\,\omega_i^{-1}.$$

The calculated moments $\langle\omega^k\rangle$ and experimental Debye Θ are presented in Table VI. Although Θ^{SP} and Θ^{B} are averages over the low-frequency region of the phonon spectrum, Θ^{SP}/Θ^{B} correlates with the calculated $\langle\omega\rangle^{SP}/\langle\omega\rangle^{B}$, which lends some support to the estimates of $\langle\omega^2\rangle^{SP}$. If these calculated values of $\langle\omega^2\rangle^{SP}$ are then used to evaluate T_c from Eq. (9) we find an increase in T_c for small lead particles while a decrease is observed (see Table VI), and the predicted enhancement of T_c for 22-Å indium is higher than the observed value. These discrepancies may be due to the nonapplicability of Eq. (9) to small particles. Many other explanations for the changes of T_c in films and small particles have been suggested but the exact mechanism is not fully understood at present.

VI. CONCLUSION

The lattice specific-heat enhancements due to low-frequency surface-phonon modes were observed in small metal particles. Decreases in the enhancements at low temperatures were interpreted as the first observation of the effect of finite size on the lattice heat capacity. An anomalously large specific-heat discontinuity was detected at the superconducting transition temperature of 22-Å indium. Possible decreases in the superconducting electronic specific heat of small lead particles were observed, and the effect of surface and size on the transition temperature were discussed.

It would be of interest to compare these experimental results of lattice behavior with realistic numerical lattice or molecular-dynamics calculations. Further experimental work on a variety of systems with different sizes and surface areas is required to establish the universal and specific features of the lattice and the electronic thermodynamic behavior in small systems.

Note added in proof. Recently H. P. Baltes and E. R. Hilf [Solid State Commun. 12, 369 (1973)] have calculated the specific heat of small (22 Å) particles using the eigenvalues of the wave equation for a free elastic vibrating sphere and obtained good agreement with the reported nonquadratic temperature dependence and maximum in the surface-phonon specific heat.

ACKNOWLEDGMENTS

The authors gratefully acknowledge the help of Dr. J. H. P. Watson and his staff who kindly pro-

vided samples. We also thank Professor E. Fawcett and Professor G. M. Graham and Dr. R. J. Birgeneau and Dr. G. P. Alldredge for helpful discussions, and R. H. Munnings and E. Latal for technical assistance.

---

*Based on Ph.D. thesis by V. Novotny (University of Toronto, 1972) (unpublished). Work supported in part by the National Research Council of Canada. One of us (V.N.) was a holder of an NRC of Canada Scholarship.

[1] A. Kh. Breger and A. A. Zhukhovitskii, Russ. J. Phys. Chem. **20**, 1459 (1946); E. W. Montroll, J. Chem. Phys. **18**, 183 (1950); R. Stratton, Philos. Mag. **44**, 519 (1953).

[2] M. Dupuis, R. Mazo, and L. Onsager, J. Chem. Phys. 33, 1452 (1960).

[3] A. A. Maradudin and R. F. Wallis, Phys. Rev. **148**, 945 (1966).

[4] R. E. Allen, G. P. Alldredge, and F. W. deWette, Phys. Rev. B **4**, 1648 (1971); Phys. Rev. B **4**, 1661 (1971).

[5] J. J. Burton, J. Chem. Phys. **52**, 345 (1970).

[6] R. E. Allen, F. W. deWette, and A. Rahman, Phys. Rev. **179**, 887 (1969); J. M. Dickey and A. Paskin, Phys. Rev. B **1**, 851 (1970).

[7] R. Kubo, J. Phys. Soc. Jap. **17**, 975 (1962).

[8] L. P. Gorkov and G. M. Eliashberg, Zh. Eksp. Teor. Fiz. 48, 1407 (1965) [Sov. Phys.-JETP 21, 940 (1965)].

[9] R. Denton, B. Mühlschlegel, and D. J. Scalapino, Phys. Rev. Lett. **26**, 707 (1971).

[10] J. A. Morrison and D. Patterson, Trans. Faraday Soc. **52**, 1 (1956).

[11] W. H. Lien and N. E. Phillips, J. Chem. Phys. **29**, 1415 (1958).

[12] T. S. Chen, G. P. Alldredge, F. W. deWette, and R. E. Allen, J. Chem. Phys. **55**, 3121 (1971).

[13] J. H. Barkman, R. L. Anderson, and J. E. Brackett, J. Chem. Phys. **42**, 1112 (1965).

[14] V. Novotny, P. P. M. Meincke, and J. H. P. Watson, Phys. Rev. Lett. **28**, 901 (1972); Proceedings of the Thirteenth International Conference on Low Temperature Physics, Boulder, Colo., 1972 (unpublished).

[15] Corning's Code No. 7930.

[16] C. G. Shull, J. Am. Chem. Soc. **70**, 1405 (1948).

[17] S. Brunauer, P. H. Emmett, and E. Teller, J. Am. Chem. Soc. **60**, 309 (1938).

[18] E. W. Washburn, Proc. Natl. Acad. Sci. USA **7**, 115 (1921).

[19] J. H. P. Watson (private communication).

[20] E. J. Korda, J. H. P. Watson, and R. H. Geiss, Micron **3**, 252 (1972).

[21] V. Novotny, T. M. Holden, and G. Dolling (unpublished).

[22] R. M. Goodman, H. H. Farrell, and G. A. Somorjai, J. Chem. Phys. **48**, 1046 (1968).

[23] J. H. P. Watson, Phys. Rev. B **2**, 1282 (1970); Phys. Rev. **148**, 223 (1966). J. Appl. Phys. **39**, 3406 (1968).

[24] V. Novotny and P. P. M. Meincke, Rev. Sci. Instrum. 44, 817 (1973).

[25] D. W. Osborne, H. E. Flotow, and F. Schreiner, Rev. Sci. Instrum. **38**, 159 (1967).

[26] J. E. Neighbor, J. F. Cochran, and C. A. Shiffman, Phys. Rev. **155**, 384 (1967).

[27] B. J. C. van der Hoeven, Jr. and P. H. Keesom, Phys. Rev. **137**, A103 (1965).

[28] M. Horowitz, A. A. Silvidi, S. F. Malaker, and J. G. Daunt, Phys. Rev. **88**, 1182 (1952).

[29] D. L. Waldorf and G. A. Alers, J. Appl. Phys. **33**, 3266 (1962).

[30] B. S. Chandrasekhar and J. A. Rayne, Phys. Rev. **124**, 1011 (1961).

[31] J. M. Vail, Can. J. Phys. **45**, 2666 (1967).

[32] S. Ewert, Z. Phys. **237**, 47 (1970).

[33] R. L. Greene, C. N. King, R. B. Zubeck, and J. J. Hauser, Phys. Rev. B **6**, 3297 (1972).

[34] A. E. H. Love, *A Treatise on the Mathematical Theory of Elasticity* (Cambridge U. P.,Cambridge, England, 1959).

[35] W. M. Rogers and R. L. Powell, Natl. Bur. Std. Circ. No. 595, 1958.

[36] NBS Special Publication No. 260-44 (1972).

[37] D. L. Decker, D. E. Mapother, and R. W. Shaw, Phys. Rev. **112**, 1888 (1958).

[38] H. R. O'Neal and N. E. Phillips, Phys. Rev. **137**, A748 (1965); C. A. Bryant and P. H. Keesom, Phys. Rev. **123**, 491 (1961); J. R. Clement and E. H. Quinnell, Phys. Rev. **92**, 258 (1953).

[39] W. L. McMillan, Phys. Rev. 167, 331 (1968).

[40] V. Novotny, Ph.D. thesis (University of Toronto, 1972) (unpublished).

[41] W. L. McMillan and J. M. Rowell, Phys. Rev. Lett. **14**, 108 (1965).

[42] R. C. Dynes, Phys. Rev. B **2**, 644 (1970).